Practical Urological Ultrasound

Pat F. Fulgham
Bruce R. Gilbert
Editors

Third Edition

Springer
MOREMEDIA

Practical Urological Ultrasound

Pat F. Fulgham • Bruce R. Gilbert
Editors

Practical Urological Ultrasound

Third Edition

Springer

Editors
Pat F. Fulgham
Department of Urology
Texas Health Presbyterian
Hospital of Dallas
Dallas, TX
USA

Bruce R. Gilbert
Zucker School of Medicine of Hofstra/
Northwell
The Arthur Smith Institute for Urology
New Hyde Park, NY
USA

ISBN 978-3-030-52308-4 ISBN 978-3-030-52309-1 (eBook)
https://doi.org/10.1007/978-3-030-52309-1

This Springer imprint is published by the registered company Springer Nature Switzerland AG
The registered company address is: Gewerbestrasse 11, 6330 Cham, Switzerland

To: The AUA National Urologic Ultrasound Faculty (NUUF) (2007–2015)
This pioneering committee of practicing urologists, organized under the auspices of the Office of Education of the American Urological Association, firmly established urologic ultrasound as an identifiable skill within the scope of the practice of urology. Owing to the efforts of the NUUF members, a generation of urologists has been educated and trained to perform safe, high-quality ultrasound examinations of their patients. The work of many of the founding members is included in this volume.

Preface

The first edition of Practical Urological Ultrasound was an outgrowth of a campaign to teach practicing urologists the basic techniques for performing and documenting ultrasound examinations on urologic patients. An emphasis on an organ-based approach was intended to mimic what was encountered in daily practice and to extend the principles learned to intraoperative applications.

The more pervasive use of MRI of the prostate for risk stratification and for MRI-guided prostate biopsy would seem to render a fundamental understanding of ultrasound less important. To the contrary, the skillful use of ultrasound is critical, not only to the co-registration of images for MRI-TRUS fusion biopsy of the prostate, but for the independent detection of the 30% of significant prostate cancers not visible on MRI. Real-time ultrasound imaging of urologic organs continues to be a mainstay of office practice and an important intraoperative aid for complex renal surgery and many prostatic procedures. Focal therapy of urological cancers will depend heavily on ultrasound guidance.

In fact, well-performed multi-parametric ultrasound (gray scale, Doppler, contrast-enhanced, elastography, and computer-enhanced) may prove to be safer, more cost-effective, and more widely available than other commonly performed axial imaging techniques. My mentor, Paul C. Peters, MD, often urged us to be responsible for "every" aspect of the care of our urologic patients. Now, with urologist-performed ultrasound, that goal is one step closer to a reality.

Central to urologist-performed imaging and imaging-based procedures is a thorough understanding of the physics underlying ultrasound imaging. We hope that this new edition will continue to enlighten urologists and encourage them to personally perform these examinations on behalf of their patients.

Dallas, TX, USA — Pat F. Fulgham
New Hyde Park, NY, USA — Bruce R. Gilbert

Acknowledgments

This book would not have been possible without the dedication and expertise of our contributing authors, many of whom are leading the way in research and developing new applications in urologic ultrasound.

Dr. Claus Roehrborn brought the practice of office-based ultrasound with him from Germany in 1983. Dr. Martin I. Resnick enlisted Claus to help educate a generation of urologists. They developed the early AUA Office of Education courses on urologic ultrasound which became the basis for much of the material in this book.

Special thanks to Dr. Bruce Gilbert whose knowledge and patience were the perfect modulating qualities for helping bind the complex pieces together into a cohesive "whole." His passion for teaching is infectious.

Angela Clark, RHIA provided invaluable assistance in manuscript preparation, image acquisition and labeling, graphics production, and research. Her talented project management, including dogged pursuit of the "finished product," has been the glue holding the project together.

Finally, thanks to my wife, Kitzi, and my children, Matt and Holly, whose forbearance permitted me the many distracted hours of writing and editing necessary to complete what proved to be a multi-year journey. It was a "task" in one sense but also a joy to see urologists take ownership of ultrasound as an invaluable tool in the management of their patients.

Dallas, TX, USA Pat F. Fulgham

The subject of this book has been a passion of mine for the past 15 years and, like many roads in life, it would not have been possible without the support and tutelage of mentors, colleagues, and friends. We dedicated the prior edition of this book to Dr. E. Darracott Vaughan my mentor and inspiration for his tireless pursuit of knowledge and his love of teaching. His continual encouragement and believing in me when I was a Post-Graduate Research Fellow in Physiology made my medical career a reality.

This book was the vision of my co-editor, colleague, and friend Dr. Pat Fulgham. Through his leadership over these past years, he has helped elevate the art of urologic ultrasound to a subspecialty within urology. He is a gifted surgeon, articulate spokesman, and tireless academician who accepts nothing less than perfection from himself, which is contagious among all that have had the great fortune to work with him.

To the authors of this book, as always, I am indebted. They continue to give tirelessly of their precious time away from family and their busy clinical practices to share their experience. Their teachings, as expressed in this text, form the basis of Urologic Ultrasound.

My wife and best friend Betsy has been the most supportive and loving partner through the late nights and endless weekends involved in the many iterations of this project. She is and has always been my source of inspiration.

New Hyde Park, NY, USA Bruce R. Gilbert

Contents

Contributors

Darian Andreas, MD Smith Institute for Urology, Northwell Health Long Island Jewish Medical Center, Lake Success, NY, USA

Tavya G. R. Benjamin, MD Zucker School of Medicine of Hofstra/ Northwell, The Arthur Smith Institute for Urology, New Hyde Park, NY, USA

Vinaya P. Bhatia, MD Texas Children's Hospital at Baylor College of Medicine, Pediatric Urology, Houston, TX, USA

Ajay Bhatnagar, RDMS Northwell Health, The Smith Institute of Urology, New Hyde Park, NY, USA

Lewis Chan, MBBS, FRACS, DDU Department of Urology, Concord Repatriation General Hospital and University of Sydney, Sydney, NSW, Australia

Akhil K. Das, MD Department of Urology, Sidney Kimmel Medical College at Thomas Jefferson University, Philadelphia, PA, USA

Rodrigo Donalisio da Silva, MD Division of Urology, Denver Health Medical Center and University of Colorado Denver, Aurora, CO, USA

Majid Eshghi, MD, FACS, MBA Department of Urology, New York Medical College, Westchester Medical Center Health, New York, NY, USA

Jason K. Frankel, MD Section of Urology and Renal Transplantation, Seattle, WA, USA

Pat F. Fulgham, MD, FACS Department of Urology, Texas Health Presbyterian Hospital of Dallas, Dallas, TX, USA

Bruce R. Gilbert, MD, PhD Zucker School of Medicine of Hofstra/ Northwell, The Arthur Smith Institute for Urology, New Hyde Park, NY, USA

Etai Goldenberg, MD Urology Consultants Ltd., Saint Louis, MO, USA

Nikhil Gupta, MD Rutgers Robert Wood Johnson Medical School, Urology, New Brunswick, NJ, USA

Dongwoon Hyun, PhD Department of Radiology, Stanford University School of Medicine, Stanford, CA, USA

Tom Jarvis, BSc, MBBS, FRACS Department of Urology, Prince of Wales Hospital and University of NSW, Sydney, NSW, Australia

Fernando J. Kim, MD, MBA, FACS Division of Urology, Denver Health Medical Center and University of Colorado Denver, Aurora, CO, USA

Zachary Kozel, MD Zucker School of Medicine at Hofstra/Northwell, The Smith Institute of Urology, New Hyde Park, NY, USA

Michael Lao, MD Division of Urology, Department of Surgery, City of Hope, Lancaster, CA, USA

Sameh Naim, MD Department of Urology, New York Medical College, Westchester Medical Center Health, New York, NY, USA

Daniel Nethala, MD Zucker School of Medicine at Hofstra/Northwell, The Smith Institute of Urology, New Hyde Park, NY, USA

Andrew Ng, MD The Smith Institute for Urology, Zucker School of Medicine of Hofstra/Northwell, New Hyde Park, NY, USA

Jeffrey S. Palmer, MD, FACS, FSPU Zucker School of Medicine at Hofstra/Northwell, Cohen Children's Medical Center of New York of the Northwell Health System, Long Island, NY, USA

Lane S. Palmer, MD, FACS, FSPU Zucker School of Medicine at Hofstra/Northwell, Division of Pediatric Urology, Northwell Health System, Long Island, NY, USA

Christopher R. Porter, MD, FACS Section of Urology and Renal Transplantation, Seattle, WA, USA

Gideon Richards, MD Department of Surgery, Banner Desert Medical Center, Arizona State Urological Institute, Chandler, AZ, USA

Daniel B. Rukstalis, MD Department of Urology, Wake Forest Baptist Medical Center, Medical Center Boulevard, Winston-Salem, NC, USA

Katherine E. Smentkowski, MD Department of Urology, Sidney Kimmel Medical College at Thomas Jefferson University, Philadelphia, PA, USA

Shannon Smith, MD The Smith Institute for Urology, Zucker School of Medicine of Hofstra/Northwell, New Hyde Park, NY, USA

Edouard J. Trabulsi, MD, FACS Department of Urology, Sidney Kimmel Medical College at Thomas Jefferson University, Philadelphia, PA, USA

Vincent Tse, MBBS, MS, FRACS Department of Urology, Concord Repatriation General Hospital and University of Sydney, Sydney, NSW, Australia

Jonathan Wagmaister, MD Department of Endourology, Soroka University Medical Center, Beer-Sheva, Israel

Thomas Williams, MD Zucker School of Medicine at Hofstra/Northwell, The Smith Institute of Urology, New Hyde Park, NY, USA

Wayland J. Wu, MD Smith Institute for Urology, Northwell Health Long Island Jewish Medical Center, Lake Success, NY, USA

History of Ultrasound

1

Vinaya P. Bhatia and Bruce R. Gilbert

Ultrasound is the portion of the acoustic spectrum characterized by sonic waves that emanate at frequencies greater than that of the upper limit of sound audible to humans, 20 kHz. A phenomenon of physics that is found throughout nature, ultrasound is utilized by rodents, dogs, moths, dolphins, whales, frogs, and bats for a variety of purposes, including communication, evading predators, and locating prey [1–4]. Lorenzo Spallazani, an eighteenth-century Italian Biologist and Physiologist, was the first to provide experimental evidence that non-audible sound exists. Moreover, he hypothesized the utility of ultrasound in his work with bats by demonstrating that bats use sound rather than sight to locate insects and avoid obstacles during flight; this was proven in an experiment where blindfolded bats were able to fly without navigational difficulty while bats with their mouths covered were not. He later determined through operant conditioning that the *Eptesicus fuscus* bat can perceive tones between 2.5 and 100 kHz [5, 6].

The human application of ultrasound began in 1880 with the work of brothers Pierre and Jacques Curie, who discovered that when pressure is applied to certain crystals, they generate electric voltage [7]. The following year, Gabriel Lippmann demonstrated the reciprocal effect, that crystals placed in an electric field become compressed [8]. The Curies demonstrated that when placed in an alternating electric current, the crystals underwent either expansion or contraction and produced high-frequency sound waves, thus creating the foundation for further work on piezoelectricity. Pierre Curie met his future wife, Marie—with whom he later shared the Nobel Prize for their work on radioactivity [9]—in 1894, when Marie was searching for a way to measure the radioactive emission of uranium salts. She turned to the piezoelectric quartz crystal as a solution, combining it with an ionization chamber and quadrant electrometer; this marked the first time piezoelectricity was used as an investigative tool [10].

The sinking of the RMS Titanic in 1912 drove the public's desire for a device capable of echolocation, or the use of sound waves to locate hidden objects. This was intensified 2 years later with the beginning of World War I, as submarine warfare became a vital part of both the Central and Allied Powers' strategies. Canadian inventor Reginald Aubrey Fessenden—perhaps most famous for his work in pioneering radio broadcasting and developing the Niagara Falls power plant—volunteered during World War I to help create an acoustic-based system for echolocation. Within

V. P. Bhatia
Texas Children's Hospital at Baylor College of Medicine, Pediatric Urology, Houston, TX, USA

B. R. Gilbert (✉)
Zucker School of Medicine of Hofstra/Northwell, The Arthur Smith Institute for Urology, New Hyde Park, NY, USA
e-mail: bgilber@northwell.edu

P. F. Fulgham, B. R. Gilbert (eds.), *Practical Urological Ultrasound*,
https://doi.org/10.1007/978-3-030-52309-1_1

3 months, he developed a high-power oscillator consisting of a 20-cm copper tube placed in a pattern of perpendicularly oriented magnetic fields that was capable of detecting an iceberg 2 miles away and being detected underwater by a receiver placed 50 miles away [11].

A contemporary of Fessenden and student of Pierre Curie, Paul Langevin was similarly interested in using acoustic technology for the detection of submarines in World War I. Using piezoelectricity, he developed an ultrasound generator in which the frequency of the alternating field was matched to the resonant frequency of the quartz crystals. This resonance evoked by the crystal produced mechanical waves that were transmitted through the surrounding medium in ultrasonic frequency and were subsequently detected by the same crystals [12, 13]. Dubbed the "hydrophone," this represented the first model of what we know today as sound navigation and ranging or SONAR. Although there were only sporadic reports on the use of SONAR in sinking German U-boats, SONAR was vital to both the Allied and Axis Powers during World War II [14].

In 1928, Russian scientist Sergei Sokolov further advanced the applicability of ultrasound in his experiments at Ulyanov Electrotechnical Institute. Using a "reflectoscope," Sokolov directed sound waves through metal objects, which were reflected at the opposite side of the object and traveled back to the reflectoscope. He determined that flaws within the metals would alter the otherwise predictable course of the sound waves. Sokolov also proposed the first "sonic camera," in which a metal's flaw could be imaged in high resolution. The actual output, however, was not adequate for practical usage. These early experiments describe what we now know as through transmission [15]. Sokolov is regarded by many as the "Father of Ultrasonics" and was awarded the Stalin prize for his work [13].

In 1936, German scientist Raimar Pohlman described an ultrasonic imaging method based on transmission via acoustic lenses, with conversion of the acoustic image into a visual entity. Two years later, Pohlman became the first to describe the use of ultrasound as a treatment modality when he observed its therapeutic effect when introduced into human tissues [16]. Austrian neurologist Karl Dussik is credited with being the first to use ultrasound as a diagnostic tool. In 1940 in a series of experiments attempting to map the human brain and potentially locate brain tumors, transducers were placed on each side of a patient's head, which along with the transducers, was partially immersed in water. At a frequency of 1.2 MHz, Dussik's "hyperphonography" was able to produce low-resolution "ventriculograms" [17]. Other investigators were unable to reproduce the same images as Dussik, sparking controversy that this may have not been true images of the cerebral ventricles, but rather, acoustic artifact. Dussik's work led MIT physician HT Ballantyne to conduct similar experiments, where they demonstrated that an empty skull produces the same images obtained by Dussik. They concluded that attenuation patterns produced by the skull were contributing to the patterns that Dussik had previously thought resulted from changes in acoustic transmission caused by the ventricles. These findings led the United States Atomic Energy Commission to conclude that ultrasound had no role in the diagnosis of brain pathology [18, 19].

In 1949, John Wild, a surgeon who had spent time in World War II treating numerous soldiers with abdominal distention following explosions, used military aviation-grade ultrasonic equipment to measure bowel thickness as a noninvasive tool to determine the need for surgical intervention. He later used A-mode comparisons of normal and cancerous tissue to demonstrate that ultrasound could be useful in the detection of cancer growth. Wild teamed up with engineer John Reid to build the first portable "echograph" for use in hospitals (Fig. 1.1) and also to develop a scanner that was capable of detecting breast and colon cancer by using pulsed waves to allow display of the location and reflectivity of an object, a mode that would later be described as "brightness mode," or simply B-mode [13, 20, 21].

Following the post–World War II resurgence of interest in cardiac surgery, Inge Edler and Hellmuth Hertz began to investigate noninvasive methods of detecting mitral stenosis, a disease with relatively poor results at the time. Using an

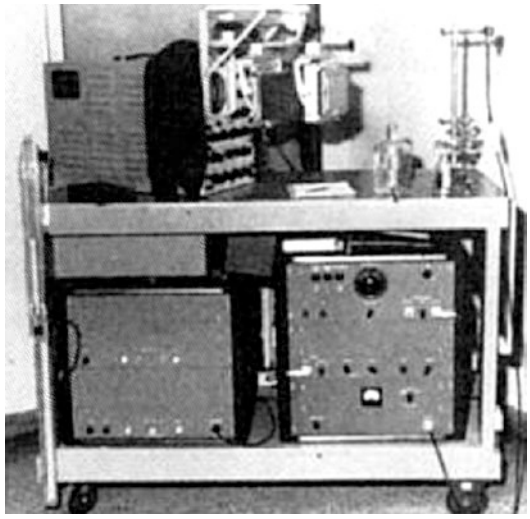

Fig. 1.1 Wild and Reid's original echograph, pictured above, was used to measure bowel thickness to determine if bowel injury had occurred and also to detect tissue thickness differences consistent with bowel and colon cancer [21]

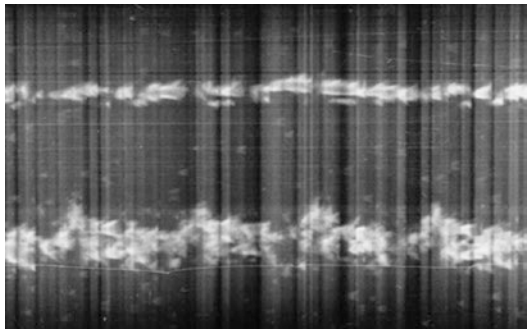

Fig. 1.2 The first echocardiographic recording is displayed as a "motion-mode," or M-mode, tracing displaying ultrasonic tracings of the left ventricular posterior wall [23]

ultrasonic reflectoscope with tracings recorded on slowly moving photographic film designed by Hertz (Fig. 1.2), they were able to capture moving structures within the heart. Dubbed "Ultrasound Cardiography," this represented the first echocardiogram, which was capable of differentiating mitral stenosis from mitral regurgitation, and detecting atrial thrombi, myxomas, and pericardial effusions [22, 23].

With the support of the Veterans Administration and United States Public Health Service, Holmes

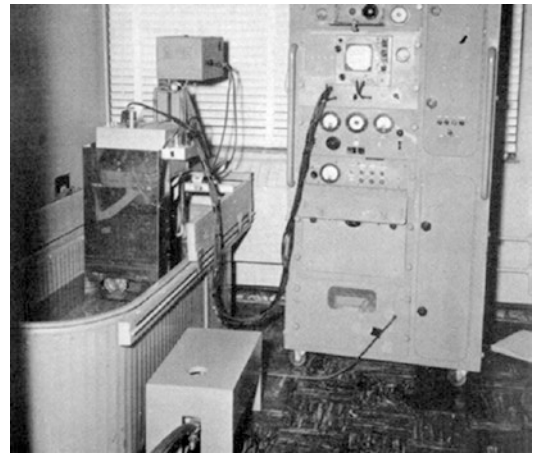

Fig. 1.3 A picture of the sonascope, as displayed, shows a large tub of liquid media in which the subject/specimen must be submerged in order for sound to travel. The oscilloscope is to the right of the tub [24]

et al. described the use of ultrasound to detect soft tissue structures with an ultrasonic "sonascope." This consisted of a large water bath in which the patient would sit, a sound generator mounted on the tub, and an oscilloscope, which would display the images (Fig. 1.3). The sonascope was capable of identifying a cirrhotic liver, renal cyst, and differentiating veins, arteries, and nerves in the neck. Consistent with the results of their predecessors, however, examinations of deeper structures, such as the pancreas, or bone penetration to evaluate the brain, proved difficult.

The use of ultrasound in obstetrics and gynecology began in 1954 when Ian Donald became interested in the use of A-mode, or amplitude-mode, which uses a single transducer to plot echoes on a screen as a function of depth; one of the early uses of this was to differentiate solid from cystic masses. Using a borrowed flaw-detector, he initially found that the patterns of the two masses were sonically unique. Working with the research department of an atomic boilermaker company, he led a team that developed the first contact scanner. Obviating the need for a large water bath, this device was hand-operated and kept in contact with skin and coupled with olive oil. Captured on Polaroid® film with an open shutter, abdominal masses could be reliably and reproducibly differentiated using ultrasound.

Three years later, Donald collaborated with his team of engineers to develop a means to measure distances on the output on a cathode ray tube, which was subsequently used to determine fetal head size [13, 24, 25].

History of Doppler Ultrasound

In 1842, Christian Johann Doppler theorized that the frequency of light received at a distance from a fixed source is different than the frequency emitted if the source is in motion [26]. More than 100 years later, this principle was applied to sound by Satomura in his study on cardiac valvular motion and peripheral blood vessel pulsation [27]. In 1958, Seattle pediatrician Rushmer and his team of engineers further advanced the technology with their development of transcutaneous continuous-wave flow measurements and spectral analysis in peripheral and extracranial brain vessels [28]. Real-time imaging—developed in 1962 by Homes—was born out of the principle of "compounding," which allowed the sonographer to sweep the transducer across the target to continuously add information to the scan; the phosphor decay displays left residual images from the prior transducer position on the screen, allowing the entire target to be visualized [13]. Siemens produced the first commercially available real-time scanner, and its first published use was in the diagnosis of hydrops fetalis [29, 30].

Bernstine and Callagan were the first to report the Obstetric utility of Doppler in their 1964 report on ultrasonic detection of fetal heart movement, thus laying the foundation for continuous fetal monitoring [31]. The same year, Buschmann was the first report "carotid echography" for the diagnosis of carotid artery thrombosis [32], although debate ensued as to whether ultrasound was capable of identifying the carotid bifurcation or its branches into the internal and external carotid arteries [33–36].

In 1966, Kato and Izumi developed a directional Doppler that was capable of determining the direction of flow [30, 37]. The following year, McLeod reported similar findings using phase-shift in the United States [30, 38]. By 1967, the use of Doppler ultrasound had spread to Europe, where continuous wave ultrasound (which does not allow precise spatial localization) was being used to diagnose occlusive disease of neck and limb arteries, venous thrombosis, and valvular insufficiency with accuracy [39]. Pulsed Doppler soon provided the capability of sampling specific Doppler signals in target tissues, a function that quickly became clinically applicable in the detection of valvular motion and differential flow rates within the heart [40].

The addition of color flow mapping to Doppler ultrasound allowed real-time mapping of blood flow patterns [41]. The limitations of color flow, including angle-dependence and difficulty assessing flow in slow-flow states, were soon appreciated. These were overcome with the advent of an alternative form of Doppler, termed "Power Doppler." This alternative to routine color flow was found to be useful in confirming or excluding difficult cases of testicular or ovarian torsion and vascular thrombosis [42].

Researchers next turned their attention to techniques to improve clarity and reduce artifacts within ultrasound-guided images. In 1980, real-time compound sonography was developed by using the probe to obtain multiple images from different viewing angles. Computed beam steering technology is then used to combine multiplanar images into one compound image in real time. Summation of these images reduced artifact and improved delineation of surfaces. This technique was expanded from linear array to curved array transducers, making it more accessible for abdominal and pelvic imaging. Now, compound sonography is used for musculoskeletal, vascular, hepatobiliary, and pelvic imaging [71].

In 1989, Baba and colleagues reported on the first production of a three-dimensional ultrasonic image. Using a real-time straight or curved transducer, they were able to obtain positional information with an ultrasound device that was connected to a microcomputer, which reconstructed the data into a three-dimensional output. The authors hypothesized that this system would be ideal for the screening of fetal anomalies and abnormalities in intrauterine growth [42]. Following the development of von Ramm's

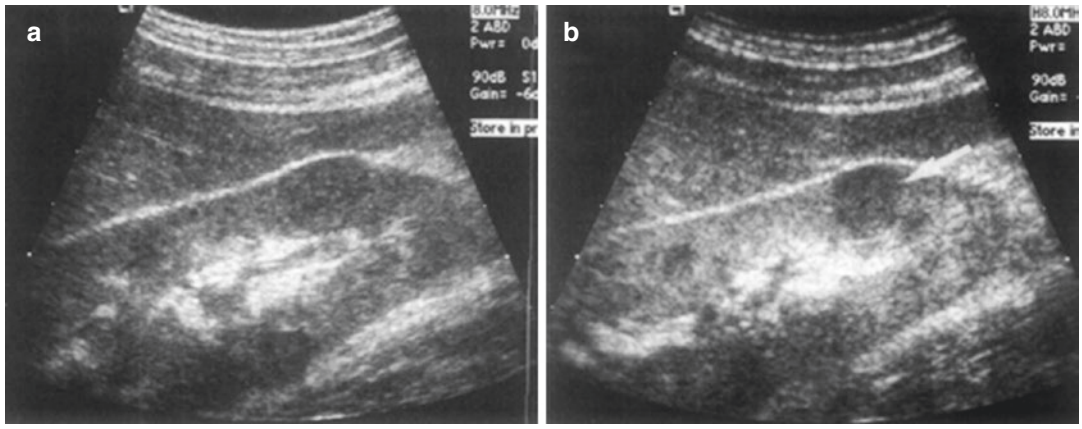

Fig. 1.4 Here, a fundamental mode image of the kidney reveals a focal contour of an abnormality seen in the lower pole (**a**), while the harmonic mode image, to the right (**b**), reveals that the lesion is solid in nature [70]

three-dimensional ultrasound device, Sheikh et al. published the first use of real-time three-dimensional acquisition and presentation of data in the United States in 1991. This proved to be useful in cardiology for the assessment of perfusion and ventricular function [43].

In 1996, several authors including Burns et al. began exploring the realm of tissue harmonic sonography (Fig. 1.4) as a means to overcome image degradation [70–71]. During the initial investigation, the authors explored microbubble ultrasound contrast media to improve contrast-agent specific images, with the result that the harmonic signal was stronger from the microbubbles than the signal from tissue. Now, harmonic mode has developed as a gray scale ultrasound mode that employs echoes at twice the transmitted frequency. This technique has resulted in improved image clarity and decreased artifact, and has proven invaluable in the diagnosis of pathology in the hepatobiliary tree and genitourinary tract, most importantly in the determining distinguishing characteristics of cystic and solid lesions.

Electronic steering of the ultrasound beam is the process of using parallel beams oriented along multiple directions from an array transducer along different directions. This is also referred to as multibeam imaging. The arrays obtained from each direction are compounded into a single image, which increases the lateral resolution and reduces the noise levels [72].

History of Ultrasound in Urology

Prostate

In 1963, Japanese Urologists Takahashi and Ouchi became the first to attempt ultrasonic examination of the prostate. However, the image quality that resulted was not interpretable and thus carried little medical utility [44]. Wild and Reid also attempted transrectal ultrasound but were met with the same result. Progress was not made until Watanabe et al. demonstrated radial scanning that could adequately identify prostate and bladder pathology. Using a purpose-built device modeled after a museum sculpture entitled "Magician's Chair," Watanabe seated his patients on a chair with a hole cut in the center such that the transducer tube could be passed through the hole and into the rectum of the seated patient [45]. Images from Watanabe's seated probe are displayed in Fig. 1.5; it is evident in Fig. 1.5b (demonstrating an area of circumscribed symmetric echogenicity, representing BPH) and Fig. 1.5c (demonstrating an asymmetric area of hyperechogenicity, representing prostate cancer) that resolution was poor and images displayed extreme contrast. Subsequent development of biplane, high-frequency probes has created increased resolution and has allowed for transrectal ultrasound to become the standard for diagnosis of prostatic disease.

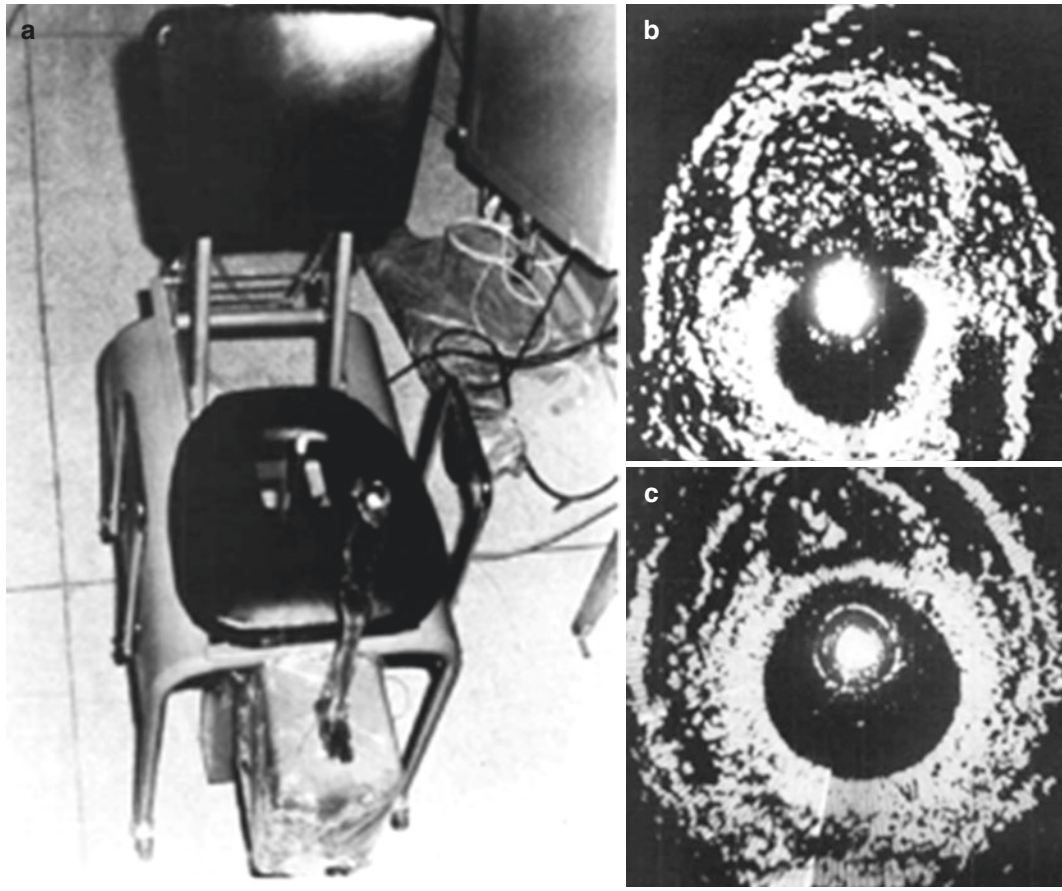

Fig. 1.5 (**a**) Images from Watanabe's seated probe are displayed [46], revealing. (**b**) an area of circumscribed symmetric echogenicity, representing BPH. (**c**) an asymmetric area of hyperechogenicity, representing prostate cancer. In these images, note that resolution was poor, and images displayed extreme contrast

In 1974, Holm and Northeved introduced a transurethral ultrasonic device that would be interchangeable with conventional optics during cystoscopy for the purpose of imaging the prostate and bladder. Their other goals for this device included the ability to determine the depth of bladder tumor penetration, prostatic volume, evaluation of prostatic tumor progression, and to assist with transurethral resection of prostate [46].

More recently, several other techniques have come to light in the diagnosis of prostate cancer.

The concept of multiparametric MRI, in which MRI images are electronically superimposed in real time on transrectal ultrasound (Fig. 1.6), has further revolutionized the ability to detect high-risk prostate cancer [67].

Histioscanning has also been used to more accurately define prostatic lesions. This involves three steps: a motorized transrectal ultrasound, a software analysis to define the region of concern, a color-coded analysis of tissue detailing all region suspicion [69].

Finally, sonoelastography, a technique for assessing tissue elasticity to distinguish cancer tissue from prostate parenchyma, has been shown to improve detection rates when ultrasound-guided biopsies alone are insufficient to define the target [68]. Sensitivity of 0.81, specificity of 0.69, and accuracy of 0.74 for detection of prostate cancer were found by Boehm et al. [74], which are similar to that of MRI.

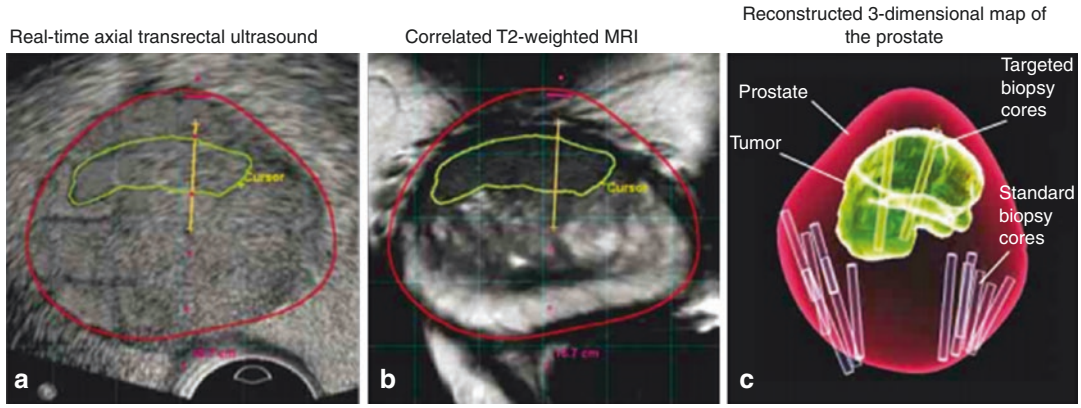

Fig. 1.6 In this example, a multiparametric MRI, T2 weighted, was obtained and outlines a suspicious lesion. Axial images (not shown) were used to demarcate a lesion suspicious for prostate cancer and marked by the radiologist prior to fusion biopsy [67]. (**a**) Next, a real-time axial ultrasound is obtained in real-time at the time of biopsy. The lesion suspicious for prostate cancer is shown in the green line, and the contour of the prostate is clarified by the red line. (**b**) The imaging platform then shows the ultrasound correlate with T2 MRI. (**c**) A post-biopsy three-dimensional map is created showing the exact location and dimension of the lesion in question

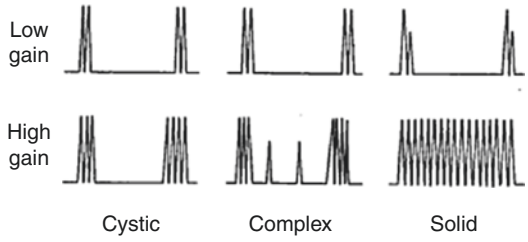

Fig. 1.7 This is a diagrammatic representation of the three types of ultrasound patterns obtained from masses. In this way, ultrasound has been able to distinguish the differences between the solid, cystic, and necrotic masses (a mixture of solid and cystic masses) [51]

Kidney and Renal Hilum

In 1971, Goldberg and Pollack, frustrated with the inability of IVP to differentiate benign from malignant lesions, turned to A-mode ultrasound. In their report on "nephrosonography," they demonstrated in a series of 150 patients the capability of ultrasound to discern solid, cystic, and complex masses with an accuracy of 96%. The diagrammatic representation of the three ultrasound patterns they found is depicted in Fig. 1.7 [47]. In cystic lesions, the first spike represents the striking of the front wall of the cyst and the second spike represents the striking of the back wall. More complex lesions, therefore, have return of more spikes.

Watanabe and colleagues demonstrated that Doppler could be used to identify the renal arteries in a noninvasive way in 1976 [48], and 5 years later, Greene and colleagues documented that Doppler could adequately differentiate stenotic from normal renal arteries [49]. In 1982, Arima et al. used Doppler to differentiate acute from chronic rejection in renal transplant patients, noting that acute rejection is characterized by the disappearance of diastolic phase, with reappearance being indicative of recovery from rejection. The authors concluded that Doppler could guide the management of rejection as an index for steroid therapy [50].

Scrotum

Perri et al. were the first to use Doppler as a sonic "stethoscope" in their workup of patients with an acute scrotum. While they were able to identify patients with epididymitis and torsion of the appendix testis as having increased flow, and patients with spermatic cord torsion as having no blood flow, they also reported that false negatives in cases of torsion could result from increased flow secondary to reactive hyperemia [51, 52].

Emerging Techniques

High-Intensity Focused Ultrasound

In the early 1990s, a number of authors investigated the therapeutic uses of high-intensity focused ultrasound or HIFU. Following prior reports of histologic changes following HIFU [53], Madersbacher and colleagues were the first to report the safety and efficacy of HIFU in symptomatic BPH patients [54]. Its utilities in the treatments of testicular cancer [55], early prostate cancer [56], recurrent prostate cancer [57], and renal cell cancer (transcutaneously [58] and laparoscopically [59]) were soon explored as well.

Elastography

Elastography, an ultrasonographic assessment of tissue stiffness has developed multiple applications across the field of urology. Because solid tumors exhibit a different tissue consistency when compared to their tissue of origin, elastography has proven useful in the assessment of prostate cancer size, location, or recurrence, and to determine the etiology of small intra-testicular lesions or degree of potential intra-testicular fibrosis in patients with varicoceles [60–62].

Histioscanning or Computer-Analyzed Ultrasound

Use of a machine-learning algorithm designed to detect concerning tissue changes evaluated in a 3D-reconstruction of ultrasound radiofrequency data [63]. However, mixed results in the imaging of prostate cancer with this technique necessitate further studies to determine its potential for future use [64].

Harmonics

Tissue harmonic imaging corrects for artifact on ultrasonography by using the higher frequency harmonic waves to generate images [65]. Documented uses for this technology included assessments of renal cysts or masses, detection of renal calculi, and improved assessment of the prostate and rectal wall [66–69].

Contrast-Enhanced Ultrasonography

In this technique, a contrast agent containing gas-filled microbubbles may be administered intravesically or intravenously prior to obtaining real-time ultrasound images. Contrast-enhanced ultrasound has gained increasing popularity in voiding cystourethrography, evaluation of prostate cancer, and defining complex renal cysts or tumors [70–72].

Multiparametric Ultrasound

Multiparametric imaging involves combining the use of any of the aforementioned ultrasound techniques to improve image quality and clarity. Several authors have explored potential implications for prostate cancer diagnosis and surveillance. Specifically, an on-going clinical trial in Germany is evaluating the combination of gray-scale ultrasound, elastography, and contrast-enhanced ultrasound to improve diagnostic yield in prostate cancer [73].

Ultrasound in Therapeutics

The field of urology continues to demand and discover novel uses for ultrasound technology. Chen et al. used transrectal ultrasound guidance to inject botulinum toxin into the external urethral sphincters of a series of patients with detrusor external sphincter dyssynergia [74]. Ozawa and colleagues used perineal ultrasound videourodynamics to accurately diagnose bladder outlet obstruction in a new, noninvasive method [75]. The possibilities for the application of ultrasound in diagnosing or treating urologic patients remain endless.

Conclusion

Ultrasound is a cost-effective, accurate, and nearly ubiquitous easy to use diagnostic tool that produces meaningful results instantly. As a standard in the urologist's office armamentarium, it can be applied to the work-up of pathology of the genitalia, pelvic floor, bladder, prostate, and kidneys. Specific uses within each organ system will be detailed throughout this book.

The history of ultrasound is quite extensive and has involved a number of ground-breaking discoveries and new applications of basic physical principles (Fig. 1.8). In the future, multiparametric imaging, multidimensional real-time ultrasound and other, yet to be developed technologies, will continue to transform the field of diagnostic medical ultrasound. This homage to the innovators of the past serves both to recognize prior achievements and to acknowledge that future work in the development of new applications for ultrasound will always be needed.

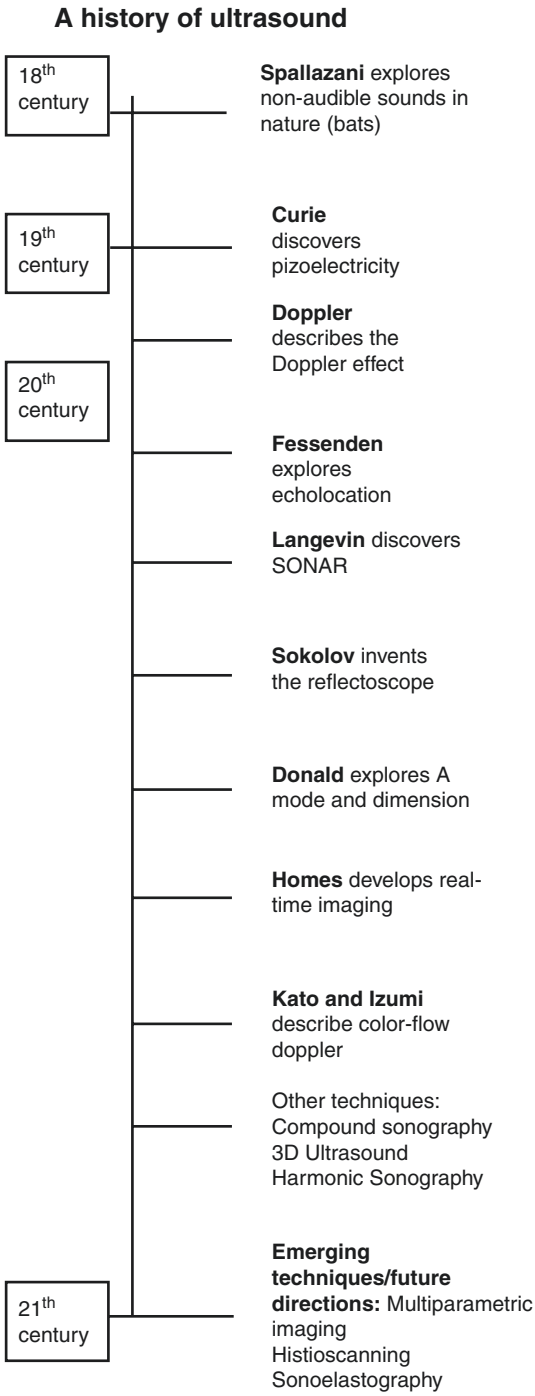

Fig. 1.8 A timeline detailing the history of important contributions to the field of ultrasonography

References

1. Corcoran A, Barber JR, Conner WE. Tiger Moth Jams Bat Sonar. Science. 2009;325(5938):325–7.
2. Dunning D, Roeder KD. Moth sounds and the insect-catching behavior of bats. Science. 1965;147:173–4.
3. Mackay RL. HM, *Dolphin Vocalization Mechanisms*. Science. 1981;212(4495):676–8.
4. Ruttimann J. Frogs chat in ultrasound. Nature News, 2006, March 15.
5. Galambos. The avoidance of obstacles by flying bats: Spallazani's ideas (1794) and later theories. Isis. 1942;34(2):132–40.
6. Dijkgraaf S. Spallanzani's unpublished experiments on the sensory basis of object perception in bats. Isis. 1960;51(1):9–20.
7. Curie JCP. Sur 'electricite polaire dans cristaux hemiedres a face inclinees. C R Seances. Acad Sci. 1880;91:383.
8. Katzir S. The discovery of the piezoelectric effect. In: The beginnings of piezoelectricity: a study in Mundane physics: Springer Nature Switzerland AG; 2006. p. 15–64.
9. Curie P. Radioactive substances, especially radium. In: Nobel Lecture; 1905, June 6.
10. Diamantis AME, Papadimitriou A, Androutsos G. The contribution of Maria Sklodowska-Curie and Pierre Curie to nuclear and medical physics. A hundred and ten years after the discovery of radium. Hell J Nucl Med. 2008;11(1):33–8.
11. Seitz F. The cosmic inventor: Reginald Aubrey Fessenden (1866-1932), vol. 89: American Philosophical Society; 1999. p. 41–6.
12. Chilowsky CLM, Procedes et appareils pour la production de signaux sous-marins diriges et pour la localisation a distance d'obstacles sous-marins. 1916.

13. Martin J. History of ultrasound. In: Resnick SRM, editor. Ultrasound in urology. Baltimore: Williams and Wilkins; 1984. p. 1–12.
14. Zimmerman D. Paul Langevin and the discovery of active sonar or asdic. North Mar. 2002;12(1):39–52.
15. Sokolov SY. The ultra-acoustic microscope. Zh Tekh Fiz. 1949;19:271.
16. Jagannathan J, et al. High-intensity focused ultrasound surgery of the brain: part 1--a historical perspective with modern applications. Neurosurgery. 2009;64(2):201–10; discussion 210-1.
17. Dussik K. Uber die Moglichkeit, hochfrequente mechanische Schwingungen als diagnostische Mittel zu verwerten. Z Ges Neurol Psych. 1941;174:153–68.
18. Thomas AMK, Banerjee AK, Busch U. Uber die Moglichkeit, hochfrequente mechanische Schwingungen als diagnostische Mittel zu verwerten. In: Banerjee AK, Thomas AMK, Busch U, editors. Classic papers in modern diagnostic radiology. Berlin: Springer; 2005. p. 144–61.
19. Shampo MA, Kyle RA. Karl Theodore Dussik--pioneer in ultrasound. Mayo Clin Proc. 1995;70(12):1136.
20. Thomas AMK, Banerjee AK, Busch U. Application of echo-ranging techniques to the determination of structure of biological tissues. In: Banerjee AK, Thomas AMK, Busch U, editors. Classic papers in modern diagnostic radiology. Berlin: Springer; 2005. p. 162–9.
21. Wild JJ, Reid JM. Application of echo-ranging techniques to the determination of structure of biological tissues. Science. 1952;115(2983):226–30.
22. Edler I, Hertz CH. The use of ultrasonic reflectoscope for the continuous recording of the movements of heart walls. 1954. Clin Physiol Funct Imaging. 2004;24(3):118–36.
23. Fraser AG. Inge Edler and the origins of clinical echocardiography. Eur J Echocardiogr. 2001;2(1):3–5.
24. Donald I, Macvicar J, Brown TG. Investigation of abdominal masses by pulsed ultrasound. Lancet. 1958;1(7032):1188–95.
25. Thomas AMK, Banerjee AK, Busch U. Investigation of abdominal masses by pulsed ultrasound. In: Banerjee AK, Thomas AMK, Busch U, editors. Classic papers in modern diagnostic radiology. Berlin: Springer; 2005. p. 213–23.
26. Doppler C. Über das farbige Licht der Doppelsterne und einiger anderer Gestirne des Himmels. Abh Königl Böhm Ges Wiss. 1843;2:465–82.
27. Satomura S. Ultrasonic Doppler method for the inspection of cardiac function. J Acoust Soc Am. 1957;29:1181–5.
28. Coman IM. Christian Andreas Doppler--the man and his legacy. Eur J Echocardiogr. 2005;6(1):7–10.
29. Hofmann D, Hollander HJ. Intrauterine diagnosis of hydrops fetus universalis using ultrasound. Zentralbl Gynakol. 1968;90(19):667–9.
30. Woo J. A short history of the development of ultrasound in obstetrics and gynecology. Available from: http://www.ob-ultrasound.net/site_index.html.
31. Bernstine RL, Callagan DA. Ultrasonic Doppler inspection of the fetal heart. Am J Obstet Gynecol. 1966;95(7):1001–4.
32. Buschmann W. On the diagnosis of carotid thrombosis. Albrecht Von Graefes Arch Ophthalmol. 1964;166:519–29.
33. Brinker RA, Landiss DJ, Croley TF. Detection of carotid artery bifurcation stenosis by Doppler ultrasound. Preliminary report. J Neurosurg. 1968;29(2):143–8.
34. Grossman BL, Wood EH. Evaluation of cerebrovascular disease utilizing a transcutaneous Doppler technic. Radiology. 1968;90(3):586–7.
35. Strandness D Jr. Ultrasonic velocity determination in the diagnosis and evaluation of peripheral vascular disease. In: Symposium on ultrasound: Indiana University; 1968.
36. Maroon JC, Campbell RL, Dyken ML. Internal carotid artery occlusion diagnosed by Doppler ultrasound. Stroke. 1970;1(2):122–7.
37. Kato KIT. A new ultrasonic flowmeter that can detect flow direction. Proceedings of the 10th scientific meeting of the Japan Society of Ultrasonics in Medicine, 1966, pp. 78–79.
38. McLeod F. A directional doppler flowmeter. Digest of the 7th international conference on medical electronics and biological engineering, 1967, p. 213.
39. Bollinger A, Partsch H. Christian Doppler is 200 years young. Vasa. 2003;32(4):225–33.
40. Baker DWJS. Doppler echocardiograpy. In: Gramiak WR, editor. Cardiac ultrasound. St. Louis: CV Mosby; 1974. p. 24.
41. Maulik D, et al. Doppler color flow mapping of the fetal heart. Angiology. 1986;37(9):628–32.
42. Hamper UM, et al. Power Doppler imaging: clinical experience and correlation with color Doppler US and other imaging modalities. Radiographics. 1997;17(2):499–513.
43. Sheikh K, et al. Real-time, three-dimensional echocardiography: feasibility and initial use. Echocardiography. 1991;8(1):119–25.
44. Takahashi HOT. The ultrasonic diagnosis in the field of urology. Proc Jpn Soc Ultrasonics Med. 1963;3:7.
45. Watanabe H, et al. Development and application of new equipment for transrectal ultrasonography. J Clin Ultrasound. 1974;2(2):91–8.
46. Holm HH, Northeved A. A transurethral ultrasonic scanner. J Urol. 1974;111(2):238–41.
47. Goldberg BB, Pollack HM. Differentiation of renal masses using A-mode ultrasound. J Urol. 1971;105(6):765–71.
48. Watanabe H, et al. Non-invasive detection of ultrasonic Doppler signals from renal vessels. Tohoku J Exp Med. 1976;118(4):393–4.
49. Greene ER, et al. Noninvasive characterization of renal artery blood flow. Kidney Int. 1981;20(4):523–9.
50. Arima M, et al. Predictability of renal allograft prognosis during rejection crisis by ultrasonic Doppler flow technique. Urology. 1982;19(4):389–94.

51. Perri AJ, et al. Necrotic testicle with increased blood flow on Doppler ultrasonic examination. Urology. 1976;8(3):265–7.
52. Perri AJ, et al. The Doppler stethoscope and the diagnosis of the acute scrotum. J Urol. 1976;116(5):598–600.
53. Burgess SE, et al. Histologic changes in porcine eyes treated with high-intensity focused ultrasound. Ann Ophthalmol. 1987;19(4):133–8.
54. Madersbacher S, et al. Tissue ablation in benign prostatic hyperplasia with high-intensity focused ultrasound. Eur Urol. 1993;23(Suppl 1):39–43.
55. Madersbacher S, et al. Transcutaneous high-intensity focused ultrasound and irradiation: an organ-preserving treatment of cancer in a solitary testis. Eur Urol. 1998;33(2):195–201.
56. Chapelon JY, et al. Treatment of localised prostate cancer with transrectal high intensity focused ultrasound. Eur J Ultrasound. 1999;9(1):31–8.
57. Berge V, Baco E, Karlsen SJ. A prospective study of salvage high-intensity focused ultrasound for locally radiorecurrent prostate cancer: early results. Scand J Urol Nephrol. 2010;44:223.
58. Kohrmann KU, et al. High intensity focused ultrasound as noninvasive therapy for multilocal renal cell carcinoma: case study and review of the literature. J Urol. 2002;167(6):2397–403.
59. Margreiter M, Marberger M. Focal therapy and imaging in prostate and kidney cancer: high-intensity focused ultrasound ablation of small renal tumors. J Endourol. 2010;24:745.
60. Wei C, et al. Prediction of postprostatectomy biochemical recurrence using quantitative ultrasound Shear wave elastography imaging. Front Oncol. 2019;9:572.
61. Fang C, Huang DY, Sidhu PS. Elastography of focal testicular lesions: current concepts and utility. Ultrasonography. 2019;38:302.
62. Erdogan H, et al. Shear wave elastography evaluation of testes in patients with Varicocele. Ultrasound Q. 2019;36:64.
63. Glybochko PV, et al. Evaluation of prostate HistoScanning as a method for targeted biopsy in routine practice. Eur Urol Focus. 2019;5(2):179–85.
64. Russo GMM, Scheepens W, et al. Angiogenesis in prostate cancer: onset, progression and imaging. BJU Int. 2012;110:E794–808.
65. Anvari A, Forsberg FSA. A primer on the physical principles of tissue harmonic imaging. Radiographics. 2015;35(7):1955.
66. Choudhry SGB, Charboneau JW, et al. Comparison of tissue harmonic imaging with conventional US in abdominal disease. Radiographics. 2000;20(4):1127–35.
67. Schmidt THC, Haage P, et al. Diagnostic accuracy of phase inversion tissue harmonic imaging versus fundamental B-mode sonography in the evaluation of focal lesions of the kidney. Am J Roentgenol. 2003;180(6):1639–47.
68. Ozdemir HDM, Temizöz O, Genchellac H, Unlu E. Phase inversion harmonic imaging improves assessment of renal calculi: a comparison with fundamental gray-scale sonography. J Clin Ultrasound. 2008;36(1):16–9.
69. Sandhu GK, Angyalfi S, Dunscombe PB, Khan RF. Is tissue harmonic ultrasound imaging (THI) of the prostatic urethra and rectum superior to brightness (B) mode imaging? An observer study. Phys Med. 2014;30(6):662–8.
70. Trabulsi EJ, et al. Prostate Contrast Enhanced Transrectal Ultrasound (CE-TRUS) evaluation of the prostate with whole mount prostatectomy correlation. Urology. 2019;133:187.
71. Ntoulia A, et al. Contrast-enhanced voiding urosonography (ceVUS) with the intravesical administration of the ultrasound contrast agent Optison for vesicoureteral reflux detection in children: a prospective clinical trial. Pediatr Radiol. 2018;48(2):216–26.
72. Dai WB, et al. Renal masses: evaluation with contrast-enhanced ultrasound, with a special focus on the Pseudocapsule sign. Ultrasound Med Biol. 2019;45(8):1924–32.
73. Mannaerts CK, et al. Multiparametric ultrasound: evaluation of greyscale, shear wave elastography and contrast-enhanced ultrasound for prostate cancer detection and localization in correlation to radical prostatectomy specimens. BMC Urol. 2018;18(1):98.
74. Boehm K, et al. Shear Wave Elastography for Localization of Prostate Cancer Lesions and Assessment of Elasticity Thresholds: Implications for Targeted Biopsies and Active Surveillance Protocols The Journal of urology. 2015;193(3):794–800. https://dx.doi.org/10.1016/j.juro.2014.09.100.
75. Ozawa H, et al. The future of urodynamics: noninvasive ultrasound videourodynamics. Int J Urol. 2010;17(3):241–9.

Physical Principles of Ultrasound

2

Pat F. Fulgham

Introduction

The use of ultrasound is fundamental to the practice of urology. In order for urologists to best use this technology on behalf of their patients, they must have a thorough understanding of the physical principles of ultrasound. Understanding how to tune the equipment and to manipulate the transducer to achieve the best-quality image is crucial to the effective use of ultrasound. The technical skills required to perform and interpret urologic ultrasound represent a combination of practical scanning ability and knowledge of the underlying disease processes of the organs being imaged. Urologists must understand how ultrasound affects biological tissues in order to use this modality safely and appropriately. When the physical principles of ultrasound are fully understood, urologists will recognize both the advantages and limitations of ultrasound.

The Mechanics of Ultrasound Waves

The image produced by ultrasound is the result of the interaction of mechanical ultrasound waves with biologic tissues and materials. Because ultrasound waves are transmitted at frequent intervals and the reflected waves received by the transducer, the images can be reconstructed and refreshed rapidly, providing a real-time image of the organs being evaluated. Ultrasound waves are "mechanical waves," which require a physical medium (such as tissue or fluid) to be transmitted. Medical ultrasound imaging utilizes frequencies in the one million cycles per second (or MHz) range. Most transducers used in urology vary from 2.5 to 29 MHz, depending on the application.

Ultrasound waves are created by applying alternating current to piezoelectric crystals within the transducer. Alternating expansion and contraction of the piezoelectric crystals create a mechanical wave, which is transmitted through a coupling medium (usually gel) to the skin and then into the body. The waves that are produced are "longitudinal waves." This means that the particle motion is in the same direction as the propagation of the wave (Fig. 2.1). This longitudinal wave produces areas of rarefaction and compression of tissue in the direction of travel of the ultrasound wave.

The compression and rarefaction of molecules are represented graphically as a sine wave alternating between a positive and negative deflection from the baseline. A "wavelength" is described as the distance between one peak of the wave and the next peak. One complete path traveled by the wave is called a "cycle." One cycle per second is known as 1 Hz (Hertz). The "amplitude" of a

P. F. Fulgham (✉)
Department of Urology, Texas Health Presbyterian Hospital of Dallas, Dallas, TX, USA
e-mail: pfulgham@airmail.net

P. F. Fulgham, B. R. Gilbert (eds.), *Practical Urological Ultrasound*,
https://doi.org/10.1007/978-3-030-52309-1_2

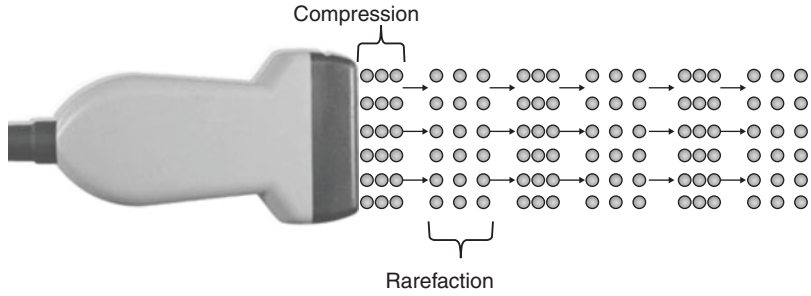

Fig. 2.1 Longitudinal waves. The expansion and contraction of piezoelectric crystals caused by the application of alternating current to the crystals causes compression and rarefaction of molecules in the tissue

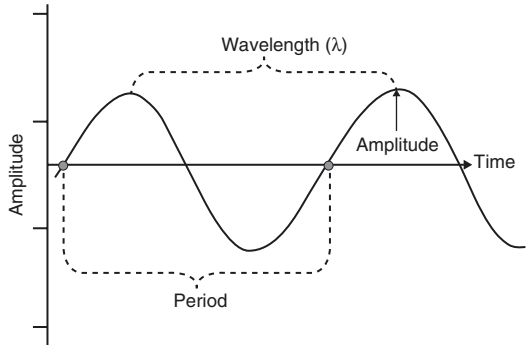

Fig. 2.2 Characteristics of a sound wave: the amplitude of the wave is a function of the acoustical power used to generate the mechanical compression wave and the medium through which it is transmitted

$$\upsilon = f\lambda$$

velocity = frequency x wavelength

Fig. 2.3 Since the velocity of sound in a given tissue is constant, the frequency and wavelength of sound must vary inversely

wave is the maximal excursion in the positive or negative direction from the baseline, and the "period" is the time it takes for one complete cycle of the wave (Fig. 2.2).

The velocity with which a sound wave travels through tissue is a product of its frequency and its wavelength. The velocity of sound in a given tissue is constant. Therefore, as the frequency of the sound wave changes, the wavelength must also change. The average velocity of sound in human tissues is 1540 m/s. The velocity of sound through a specific tissue is related to the density of the tissue. Wavelength and frequency vary in an inverse relationship. Velocity equals frequency times wavelength (Fig. 2.3). As the frequency diminishes from 10 to 1 MHz, the wavelength increases from 0.15 to 1.5 mm. This has important implications for the choice of transducer depending on the indication for imaging.

Ultrasound Image Generation

The image produced by an ultrasound machine begins with the transducer. "Transducer" comes from the Latin "transducere," which means to convert. In this case, electrical impulses are converted to mechanical sound waves via the "piezoelectric effect."

In ultrasound imaging, the transducer has a dual function as a "sender" and a "receiver." Sound waves are transmitted into the body where they are at least partially reflected. The piezoelectric effect occurs when alternating current is applied to a crystal containing dipoles [1]. Areas of charge within a piezoelectric element are distributed in patterns, which yield a "net" positive and negative orientation. When alternating charge is applied to the two opposite faces of the piezoelectric element, a relative contraction or elongation of the charged areas occurs resulting in a mechanical expansion and then a contraction of the element. This results in a mechanical wave that is transmitted to the patient (Fig. 2.4).

Reflected mechanical sound waves are received by the transducer and converted back into electrical energy via the piezoelectric effect. The electrical energy is interpreted within the ultrasound instrument to generate an image which is displayed upon the screen.

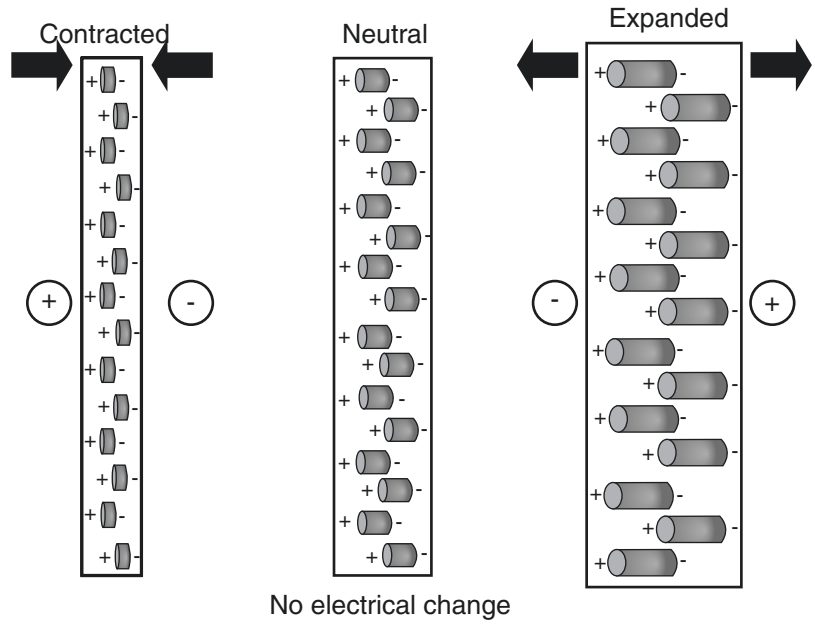

Fig. 2.4 Piezoelectric effect. Areas of "net" charge within a crystal expand or contract when current is applied to the surface, creating a mechanical wave. When the returning mechanical wave strikes the crystal, an electrical current is generated

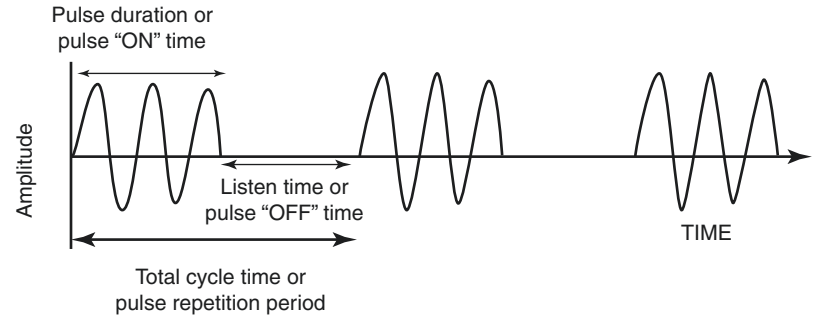

Fig. 2.5 The pulsed-wave ultrasound mode depends on an emitted pulse of 2–4 wave cycles followed by a period of "silence" as the transducer awaits the return of the emitted pulse

For most modes of ultrasound, the transducer emits a limited number of wave cycles (usually two to four) called a pulse. The frequency of the two to four waves within each cycle is usually in the 2.5–14 MHz range. The transducer is then "silent" as it awaits the return of the reflected waves from within the body (Fig. 2.5). The transducer serves as a receiver more than 99% of the time.

Pulses are sent out at regular intervals usually between 1 and 10 kHz, which is known as the "pulse repetition frequency" (PRF). By timing the pulse from transmission to reception, it is possible to calculate the distance from the transducer to the object reflecting the wave. This is known as "ultrasound ranging" (Fig. 2.6). This sequence is known as "pulsed-wave ultrasound."

The amplitude of the returning waves determines the brightness of the pixel assigned to the reflector in an ultrasound image. The greater the amplitude of the returning wave, the brighter the pixel assigned. Thus, an ultrasound unit produces an "image" by first causing a transducer to emit a series of ultrasound waves at specific frequencies and intervals and then interpreting the returning echoes for the duration of transit and amplitude. This "image" is rapidly refreshed on a monitor to give the impression of continuous motion. Frame refresh rates are typically 12–30 per second. The sequence of events depicted in Fig. 2.7 is the basis for all "scanned" modes of ultrasound including the familiar gray-scale ultrasound.

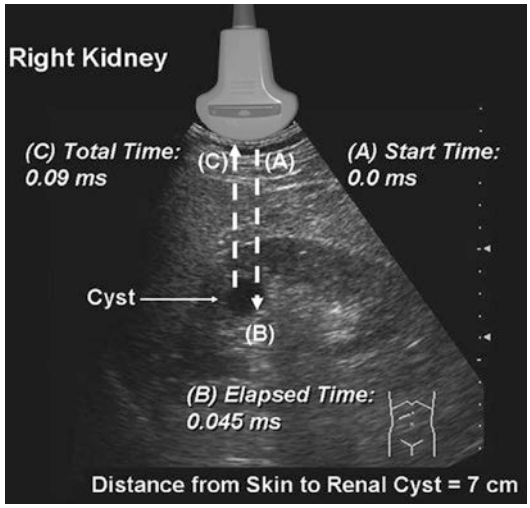

Fig. 2.6 Ultrasound ranging depends on assumptions about the average velocity of ultrasound in human tissue to locate reflectors in the ultrasound field. The elapsed time from pulse transmission to reception of the same pulse by the transducer allows for determining the location of a reflector in the ultrasound field

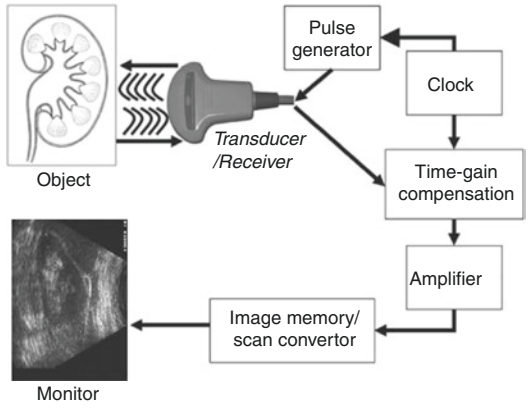

Fig. 2.7 Schematic depiction of the sequence of image production by an ultrasound device

Interaction of Ultrasound with Biological Tissue

As ultrasound waves are transmitted through human tissue, they are altered in a variety of ways including loss of energy, change of direction, and change of frequency. An understanding of these interactions is necessary to maximize image quality and correctly interpret the resultant images.

Attenuation refers to a loss of kinetic energy as a sound wave interacts with tissues and fluids within the body [2]. Specific tissues have different potentials for attenuation. For example, water has an attenuation of 0.0, whereas kidney has an attenuation of 1.0 and muscle an attenuation of 3.3. Therefore, sound waves are much more rapidly attenuated as they pass through muscle than as they pass through water (Fig. 2.8). (Attenuation is measured in dB/cm/MHz.)

The three most important mechanisms of attenuation are absorption, reflection, and scattering. Absorption occurs when the mechanical kinetic energy of a sound wave is converted to heat within the tissue. Absorption is dependent on the frequency of the sound wave and the characteristics of the attenuating tissue. Higher frequency waves are more rapidly attenuated by absorption than lower frequency waves.

Since sound waves are progressively attenuated with distance traveled, deep structures in the body (e.g., kidney) are more difficult to image. Compensation for loss of acoustic energy by attenuation can be accomplished by the appropriate use of gain settings (increasing the sensitivity of the transducer to returning sound waves) and selection of a lower frequency.

Refraction occurs when a sound wave encounters an interface between two tissues at any angle other than 90°. When the wave strikes the interface at an angle, a portion of the wave is reflected and a portion transmitted into the adjacent media. The direction of the transmitted wave is altered (refracted). This results in a loss of some information because the wave is not completely reflected back to the transducer but also causes potential errors in registration of object location because of the refraction (change in direction) of the wave. The optimum angle of insonation to minimize attenuation by refraction is 90° (Fig. 2.9).

Reflection occurs when sound waves strike an object or an interface between unlike tissues or structures. If the object has a relatively large flat surface, it is called a specular reflector, and sound waves are reflected in a predictable way based on the angle of insonation. If a reflector is small or irregular, it is called a diffuse reflector. Diffuse

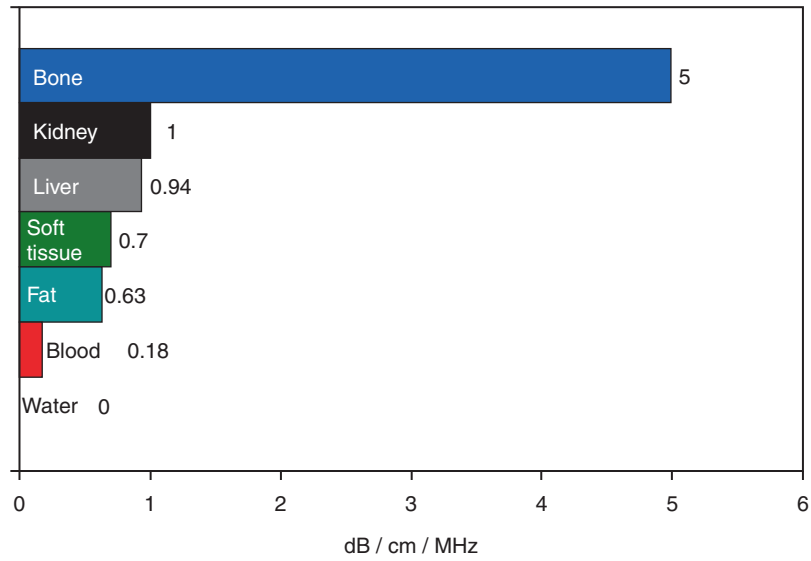

Fig. 2.8 Attenuation of tissue. (Adapted from Diagnostic Ultrasound, Third Ed., Vol 1). The attenuation of a tissue is a measure of how the energy of an ultrasound wave is dissipated by that tissue. The higher the attenuation value of a tissue, the more the sound wave is attenuated by passing through that tissue

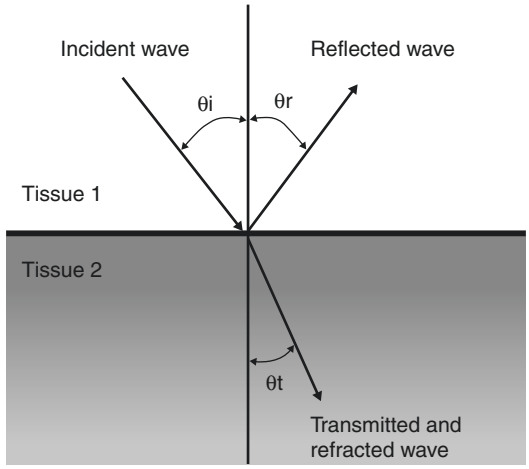

Fig. 2.9 A wave which strikes the interface between two tissues of differing impedance is usually partially reflected and partially transmitted with refraction. A portion of the wave is reflected at an angle (θr) equal to the angle of insonation (θi); a portion of the wave is transmitted at a refracted angle (θt) into the second tissue

reflectors produce *scattering* in a pattern, which produces interference with waves from adjacent diffuse reflectors. The resulting pattern is called "speckle" and is characteristic of solid organs such as the testes and liver (Fig. 2.10).

When a sound wave travels from one tissue to another, a certain amount of energy is reflected at the interface between the tissues. The percentage of energy reflected is a function of the difference in the "impedance" of the tissues. Impedance is a property of tissue related to its "stiffness" and the speed at which sound travels through the tissue [3]. If two adjacent tissues have a small difference in tissue impedance, very little energy will be reflected. The impedance difference between kidney (1.63) and liver (1.64) is very small so that if these tissues are immediately adjacent, it may be difficult to distinguish the interface between the two by ultrasound (Table 2.1).

Fat has a sufficient impedance difference from both kidney and liver that the borders of the two organs can be distinguished from the intervening fat (Fig. 2.11).

If the impedance differences between tissues are very high, complete reflection of sound waves may occur, resulting in acoustic shadowing (Fig. 2.12).

Artifacts

Sound waves are emitted from the transducer with a known amplitude, direction, and frequency. Interactions with tissues in the body result in alterations of these parameters. Returning sound waves are presumed to have undergone alterations according to the expected physical principles such as attenuation with distance and frequency shift based on the velocity

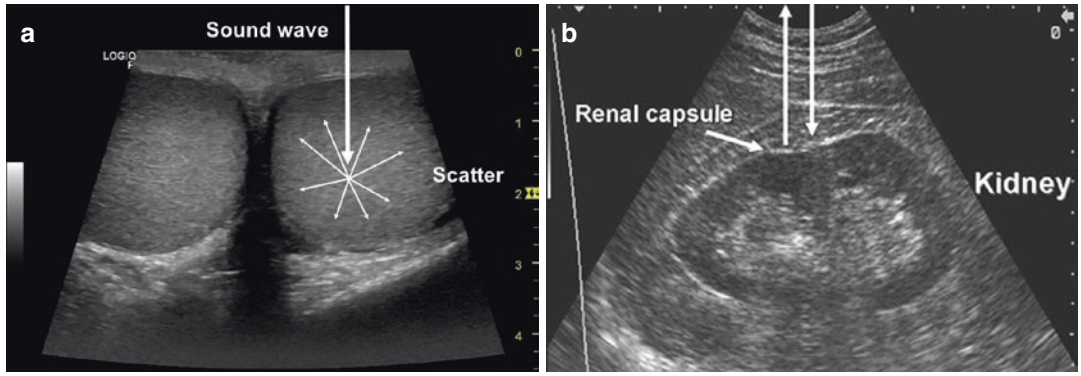

Fig. 2.10 (**a**) Demonstrates a diffuse reflector. In this simultaneous bilateral view of the testes, small parenchymal structures scatter sound waves. The pattern of interference resulting from this scattering provides the familiar "speckled" pattern of testicular echo architecture. (**b**) Demonstrates a specular reflector. A specular reflector reflects sound waves at an angle equal to the incident angle without producing a pattern of interference caused by scattering. In this image of the kidney, the capsule of the kidney serves as a specular reflector

Table 2.1 Impedance of tissue

Tissue	Density (kg/m^3)	Impedance (Rayles)
Air and other gases	1.2	0.0004
Fat tissue	952	1.38
Water and other clear liquids	1000	1.48
Kidney (average of soft tissue)	1060	1.63
Liver	1060	1.64
Muscle	1080	1.70
Bone and other calcified objects	1912	7.8

Adapted from Diagnostic Ultrasound, 3rd Ed, Vol. 1
Impedance (Z) is a product of tissue density (p) and the velocity of sound in that tissue (c). Impedance is defined by the formula: Z (Rayles) = p (kg/m^3) × c (m/s)

and direction of objects they encountered. The timing of the returning echoes is based on the expected velocity of sound in human tissue. When these expectations are not met, it may lead to image representations and measurements, which do not reflect actual physical conditions. These misrepresentations are known as "artifacts." Artifacts, if correctly identified, can be used to aid in diagnosis.

Increased through-transmission occurs when sound waves pass through tissue with less attenuation than the surrounding tissue. For example, when sound waves pass through a fluid-filled structure such as a renal cyst, the waves experience relatively little attenuation compared to that experienced in the surrounding renal parenchyma. Thus, when the waves reach the posterior wall of the cyst and the renal tissue beyond it, they are more energetic (have greater amplitude) than the adjacent waves. The returning echoes have significantly greater amplitude than waves returning through the renal parenchyma from the same region of the kidney. Therefore, the pixels associated with the region distal to the cyst are assigned a greater "brightness." The tissue appears hyperechoic compared to the adjacent peri-renal tissue even though it is histologically identical (Fig. 2.13). This artifact can be overcome by changing the angle of insonation or adjusting the time-gain compensation settings.

Acoustic shadowing occurs when there is significant attenuation of sound waves at a tissue interface causing loss of information about other structures distal to that interface. This attenuation may occur on the basis of reflection or absorption, resulting in an "anechoic" or "hypoechoic" shadow. The significant attenuation or loss of the returning echoes from tissues distal to the interface may lead to incorrect conclusions about tissue in that region. For instance, when sound waves strike the interface between testicular tissue and a testicular calcification, there is a large impedance difference and significant attenuation and reflection occur. Information about the region distal to the interface is therefore lost or severely diminished (Fig. 2.14). Thus, in some cases spherical objects may appear as crescenteric objects, and it may be difficult to obtain accurate

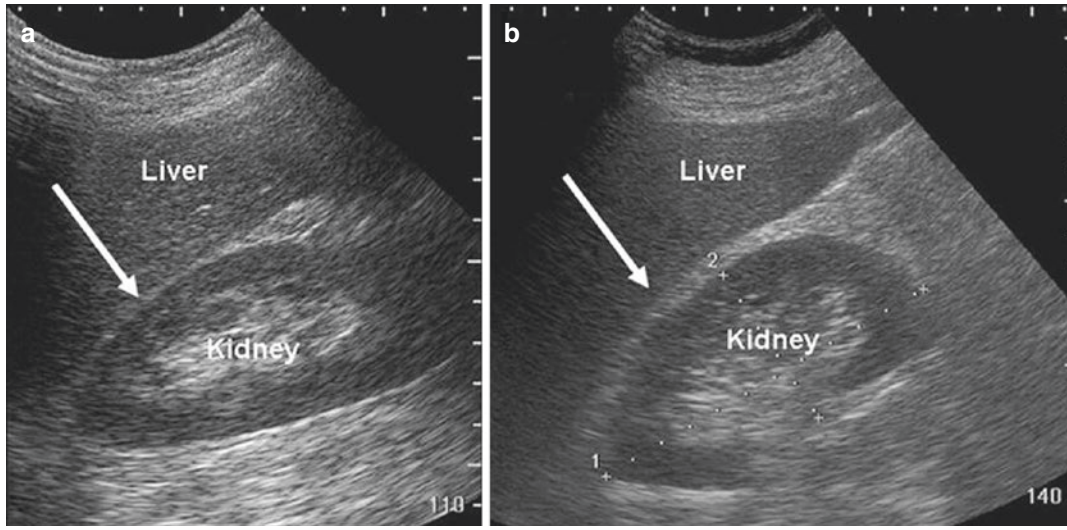

Fig. 2.11 Image (**a**) demonstrates that when the kidney and liver are directly adjacent to each other, it is difficult to appreciate the boundary (*arrow*) between the capsules of the kidney and liver. Image (**b**) demonstrates that when fat (which has a significantly lower impedance) is interposed, it is far easier to appreciate the boundary between liver capsule (*arrow*) and fat

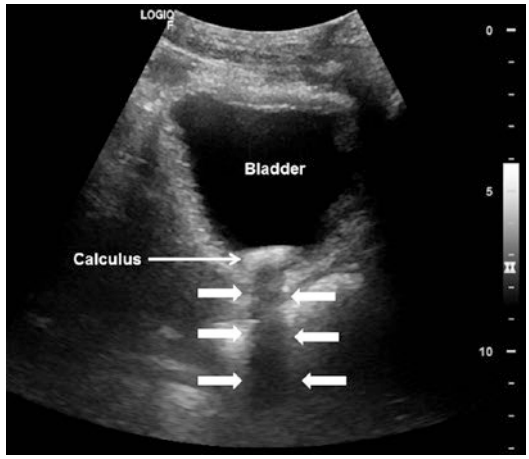

Fig. 2.12 In the urinary bladder, reflection of sound waves as the result of large impedance differences between urine and the bladder calculus. Acoustic shadowing results from nearly complete reflection of sound waves (*arrows*)

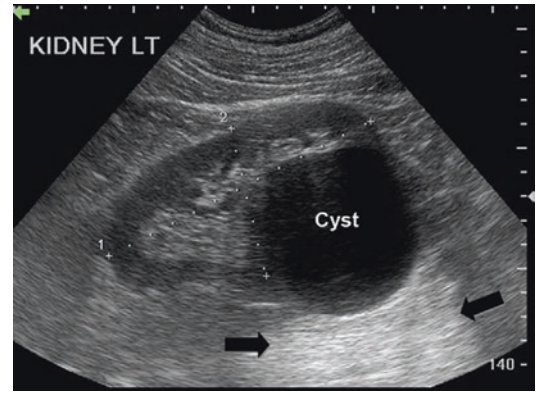

Fig. 2.13 Increased through-transmission with hyperechogenicity (*arrow*) as the result of decreased attenuation by the fluid-filled cyst. This is an example of artifactual misrepresentation of tissue characteristics and must be recognized to avoid incorrect clinical conclusions

measurements of such three-dimensional objects. Furthermore, fine detail in the region of the acoustic shadow may be obscured. The problems with acoustic shadowing are most appropriately overcome by changing the angle of insonation.

Edging artifact occurs when sound waves strike a curved surface or an interface at a critical angle. A "critical angle" of insonation is one which results in propagation of the sound wave along the interface without significant reflection of the wave to the transducer. Thus, information distal to the interface is lost or severely diminished. This very common artifact in urology must